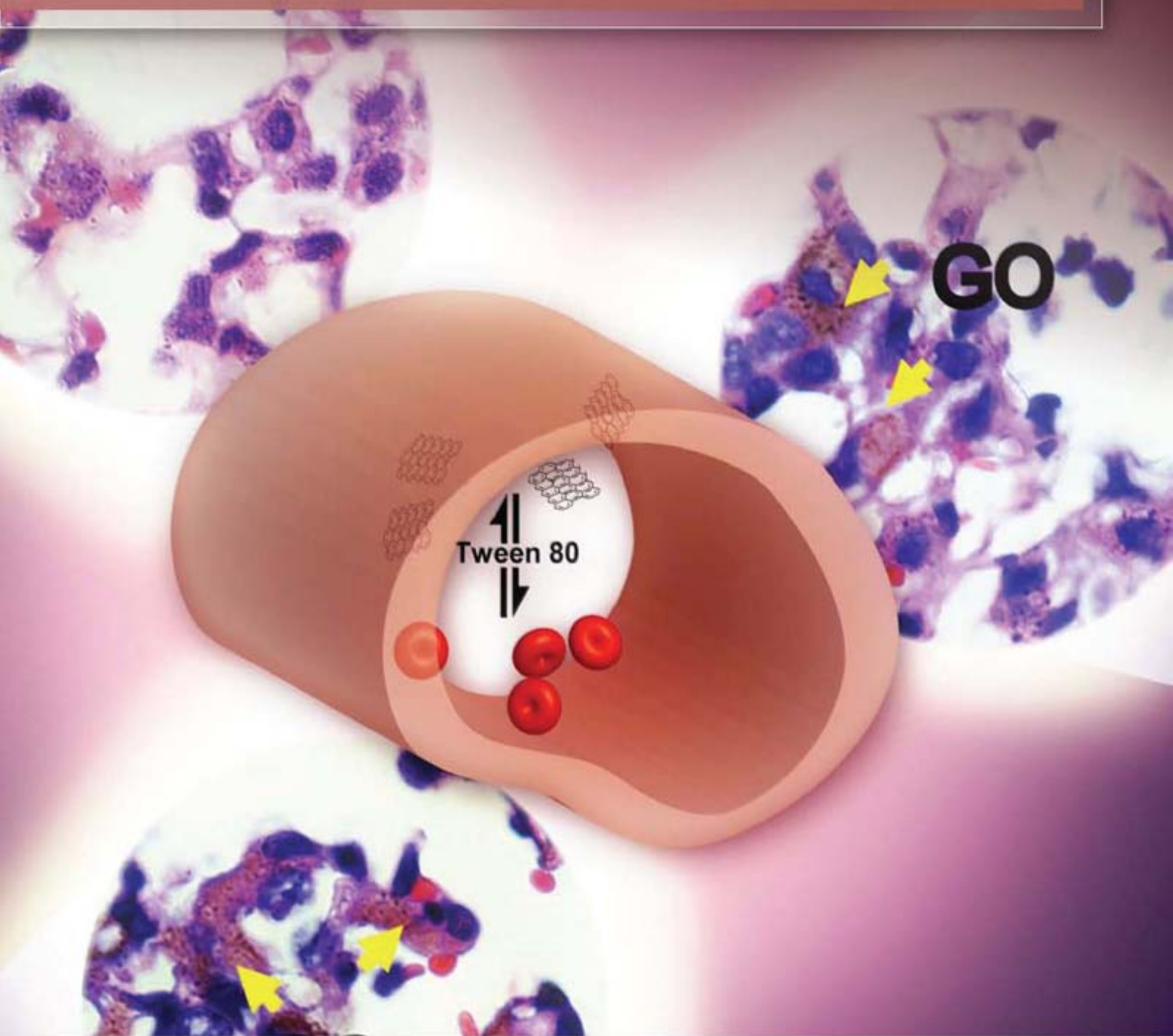


JES

JOURNAL OF
ENVIRONMENTAL
SCIENCES

ISSN 1001-0742
CN 11-2529/X

May 1, 2013 Volume 25 Number 5
www.jesc.ac.cn



Sponsored by
Research Center for Eco-Environmental Sciences
Chinese Academy of Sciences

CONTENTS

Environmental biology

Continuous live cell imaging of cellulose attachment by microbes under anaerobic and thermophilic conditions
using confocal microscopy

Zhi-Wu Wang, Seung-Hwan Lee, James G. Elkins, Yongchao Li, Scott Hamilton-Brehm, Jennifer L. Morrell-Falvey 849

Response of anaerobes to methyl fluoride, 2-bromoethanesulfonate and hydrogen during acetate degradation

Liping Hao, Fan Lü, Lei Li, Liming Shao, Pinjing He 857

Effect of airflow on biodrying of gardening wastes in reactors

F. J. Colomer-Mendoza, L. Herrera-Prats, F. Robles-Martínez, A. Gallardo-Izquierdo, A. B. Piña-Guzmán 865

Environmental health and toxicology

The *ex vivo* and *in vivo* biological performances of graphene oxide and the impact of surfactant on graphene
oxide's biocompatibility (Cover story)

Guangbo Qu, Xiaoyan Wang, Qian Liu, Rui Liu, Nuoya Yin, Juan Ma, Liquan Chen, Jiuyang He, Sijin Liu, Guibin Jiang 873

Determination of the mechanism of photoinduced toxicity of selected metal oxide nanoparticles (ZnO, CuO, Co₃O₄ and
TiO₂) to *E. coli* bacteria

Thabitha P. Dasari¹, Kavitha Pathakoti², Huey-Min Hwang 882

Joint effects of heavy metal binary mixtures on seed germination, root and shoot growth, bacterial bioluminescence,
and gene mutation

In Chul Kong 889

Atmospheric environment

An online monitoring system for atmospheric nitrous acid (HONO) based on stripping coil and ion chromatography

Peng Cheng, Yafang Cheng, Keding Lu, Hang Su, Qiang Yang, Yikan Zou, Yanran Zhao,

Huabing Dong, Limin Zeng, Yuanhang Zhang 895

Formaldehyde concentration and its influencing factors in residential homes after decoration at Hangzhou, China

Min Guo, Xiaoqiang Pei, Feifei Mo, Jianlei Liu, Xueyou Shen 908

Aquatic environment

Flocculating characteristic of activated sludge flocs: Interaction between Al³⁺ and extracellular polymeric substances

Xiaodong Ruan, Lin Li, Junxin Liu 916

Speciation of organic phosphorus in a sediment profile of Lake Taihu II. Molecular species and their depth attenuation

Shiming Ding, Di Xu, Xiuling Bai, Shuchun Yao, Chengxin Fan, Chaosheng Zhang 925

Adsorption of heavy metal ions from aqueous solution by carboxylated cellulose nanocrystals

Xiaolin Yu, Shengrui Tong, Maofa Ge, Lingyan Wu, Junchao Zuo, Changyan Cao, Weiguo Song 933

Synthesis of mesoporous Cu/Mg/Fe layered double hydroxide and its adsorption performance for arsenate in aqueous solutions

Yanwei Guo, Zhiliang Zhu, Yanling Qiu, Jianfu Zhao 944

Advanced regeneration and fixed-bed study of ammonium and potassium removal from anaerobic digested wastewater
by natural zeolite

Xuejun Guo, Larry Zeng, Xin Jin 954

Eutrophication development and its key regulating factors in a water-supply reservoir in North China	
Liping Wang, Lusan Liu, Binghui Zheng	962
Laboratory-scale column study for remediation of TCE-contaminated aquifers using three-section controlled-release potassium permanganate barriers	
Baoling Yuan, Fei Li, Yanmei Chen, Ming-Lai Fu	971
Influence of Chironomid Larvae on oxygen and nitrogen fluxes across the sediment-water interface (Lake Taihu, China)	
Jingge Shang, Lu Zhang, Chengjun Shi, Chengxin Fan	978
Comparison of different phosphate species adsorption by ferric and alum water treatment residuals	
Sijia Gao, Changhui Wang, Yuansheng Pei	986
Removal efficiency of fluoride by novel Mg-Cr-Cl layered double hydroxide by batch process from water	
Sandip Mandal, Swagatika Tripathy, Tapswani Padhi, Manoj Kumar Sahu, Raj Kishore Patel	993
Determining reference conditions for TN, TP, SD and Chl- <i>a</i> in eastern plain ecoregion lakes, China	
Shouliang Huo, Beidou Xi, Jing Su, Fengyu Zan, Qi Chen, Danfeng Ji, Chunzi Ma	1001
Nitrate in shallow groundwater in typical agricultural and forest ecosystems in China, 2004–2010	
Xinyu Zhang, Zhiwei Xu, Xiaomin Sun, Wenyi Dong, Deborah Ballantine	1007
Influential factors of formation kinetics of flocs produced by water treatment coagulants	
Chunde Wu, Lin Wang, Bing Hu, Jian Ye	1015
Environmental catalysis and materials	
Characterization and performance of Pt/SBA-15 for low-temperature SCR of NO by C ₃ H ₆	
Xinyong Liu, Zhi Jiang, Mingxia Chen, Jianwei Shi, Wenfeng Shangguan, Yasutake Teraoka	1023
Photo-catalytic decolourisation of toxic dye with N-doped titania: A case study with Acid Blue 25	
Dhruba Chakraborty, Susmita Sen Gupta	1034
Pb(II) removal from water using Fe-coated bamboo charcoal with the assistance of microwaves	
Zengsheng Zhang, Xuejiang Wang, Yin Wang, Siqing Xia, Ling Chen, Yalei Zhang, Jianfu Zhao	1044
Serial parameter: CN 11-2629/X*1989*m*205*en*P*24*2013-5	



Adsorption of heavy metal ions from aqueous solution by carboxylated cellulose nanocrystals

Xiaolin Yu¹, Shengrui Tong^{1,*}, Maofa Ge^{1,*}, Lingyan Wu¹,
Junchao Zuo¹, Changyan Cao², Weiguo Song²

1. Beijing National Laboratory for Molecular Sciences, State Key Laboratory for Structural Chemistry of Unstable and Stable Species, Institute of Chemistry, Chinese Academy of Sciences, Beijing 100190, China

2. Laboratory for Molecular Nanostructures and Nanotechnology, Institute of Chemistry, Chinese Academy of Sciences, Beijing 100190, China

Received 10 August 2012; revised 20 November 2012; accepted 03 December 2012

Abstract

A novel nanoadsorbent for the removal of heavy metal ions is reported. Cotton was first hydrolyzed to obtain cellulose nanocrystals (CNCs). CNCs were then chemically modified with succinic anhydride to obtain SCNCs. The sodic nanoadsorbent (NaSCNCs) was further prepared by treatment of SCNCs with saturated NaHCO_3 aqueous solution. Batch experiments were carried out with SCNCs and NaSCNCs for the removal of Pb^{2+} and Cd^{2+} . The effects of contact time, pH, initial adsorption concentration, coexisting ions and the regeneration performance were investigated. Kinetic studies showed that the adsorption equilibrium time of Pb^{2+} and Cd^{2+} was reached within 150 min on SCNCs and 5 min on NaSCNCs. The adsorption capacities of Pb^{2+} and Cd^{2+} on SCNCs and NaSCNCs increased with increasing pH. The adsorption isotherm was well fitted by the Langmuir model. The maximum adsorption capacities of SCNCs and NaSCNCs for Pb^{2+} and Cd^{2+} were 367.6 mg/g, 259.7 mg/g and 465.1 mg/g, 344.8 mg/g, respectively. SCNCs and NaSCNCs showed high selectivity and interference resistance from coexisting ions for the adsorption of Pb^{2+} . NaSCNCs could be efficiently regenerated with a mild saturated NaCl solution with no loss of capacity after two recycles. The adsorption mechanisms of SCNCs and NaSCNCs were discussed.

Key words: cellulose nanocrystals; adsorption; isotherms; regeneration

DOI: 10.1016/S1001-0742(12)60145-4

Introduction

Pollution by heavy metals, due to their toxic nature and other adverse effects, is one of the most serious environmental problems (Anirudhan and Sreekumari, 2011). Many heavy metal ions, such as lead, cadmium, copper, and mercury, are detected in industrial wastewaters originating from metal plating, mining activities, paint manufacture, etc. These heavy metals are not biodegradable and tend to accumulate in living organisms, causing various diseases and disorders (Lu et al., 2010). Therefore, they must be removed from aqueous solution before discharge.

Among these heavy metal ions, lead and cadmium are the most toxic (Musyoka et al., 2011). These heavy metal ions pose serious health implications to the vital organs of human beings and animals when consumed above certain threshold concentrations. At high exposure levels, lead

causes encephalopathy, cognitive impairment, behavioral disturbances, kidney damage, anemia, and toxicity to the reproductive system (Pagliuca et al., 1990); and cadmium is associated with nephrotoxic effects and bone damage (Friberg, 1985). According to the World Health Organization criteria, the permissible limits of lead and cadmium in wastewater are 0.015 mg/L and 0.01 mg/L, respectively (Musyoka et al., 2011).

Conventional methods, including physical and chemical processes, have been used to remove heavy metal ions from water, such as ion exchange (Nada and Hassan, 2006), chemical precipitation (Esalah et al., 2000), reverse osmosis (Li et al., 2007), membrane separation (Canet et al., 2002), electrochemical techniques (Chen et al., 2002b) and biosorption (Ma et al., 2010; Xing et al., 2011). However, most of these methods have high operating cost and the need for disposal of the resulting solid waste. Due to the advantages of economical feasibility and environmental friendly behavior, adsorption is regarded as the best technique for removing heavy metal ions (O'Connell et al.,

* Corresponding author: E-mail: gemaofa@iccas.ac.cn (Maofa Ge); tongsr@iccas.ac.cn (Shengrui Tong)

2008).

Cellulose, the most widely available and renewable biopolymer in nature, is a very promising raw material available at low cost for the preparation of various functional materials. Native cellulose may be categorized as a semicrystalline fibrillar material, which is constituted of amorphous and crystalline regions. The amorphous regions act as structural defects and are susceptible to acid attack, and then individual short monocrystalline nanoparticles called cellulose nanocrystals (CNCs) are released. The length and lateral dimension of cellulose nanocrystals are reported to be around 200 nm and 5 nm (Samir et al., 2005), respectively. The small size results in a high aspect ratio and a large specific surface area. Because of the chemical structure of cellulose, the CNC surface bears numerous hydroxyl groups, which leads to high activity and the ability to react with various specific groups (Hasani et al., 2008; Kloser and Gray, 2010). Due to high specific surface areas and numerous reactive groups, excellent adsorption performance may be obtained with modified CNCs. Therefore, after modification with functional groups such as amino groups (da Silva Filho et al., 2009; Shen et al., 2009), sulfonic acid groups (Güçlüet al., 2003), and carboxyl groups (Karnitz et al., 2010; Li et al., 2010; Zhao et al., 2011), CNCs are able to remove heavy metal ions from aqueous solution with relatively high adsorption capacity.

Succinic anhydride is widely used in the manufacture of agrochemicals, dyes, photographic chemicals, surface active agents, lubricant additives, organic flame retardant materials, esters, flavors and fragrances. It is produced by two COOH groups of succinic acid combining with the loss of a water molecule. Therefore, succinic anhydride is an active agent containing one anhydride group, which can react with the hydroxyl groups of cellulose. In recent decades, there have been many investigations concerning the modification of cellulose with succinic anhydride for the removal of heavy metal ions (Belhafaoui et al., 2009; Gurgel and Gil, 2009; Karnitz et al., 2007). However, modification of CNCs with succinic anhydride, to our knowledge, has not been reported till now.

In this study, CNCs were first prepared by sulfuric acid hydrolysis of cotton. Subsequently, CNCs were modified with succinic anhydride, and the product SCNCs were then converted into the sodic form (NaSCNCs). SCNCs and NaSCNCs were used to remove the Pb^{2+} and Cd^{2+} from aqueous solution. The effects of contact time, pH, initial adsorption concentration, coexisting ions and the regeneration performance were investigated. Furthermore, the adsorption mechanism was systematically investigated.

1 Materials and methods

1.1 Materials

Medical absorbent cotton was obtained from Jiaozuo League Hygiene Group (China). Succinic anhydride,

$\text{Pb}(\text{NO}_3)_2$, CdCl_2 were purchased from Aladdin Reagent Co., Ltd. Pyridine, $\text{Mg}(\text{NO}_3)_2$, $\text{Ca}(\text{NO}_3)_2$ and KNO_3 were purchased from Sinopharm Chemical Reagent Co., Ltd. Pyridine was refluxed with NaOH and distilled to remove trace water. All other solvents and reagents were used without further purification.

1.2 Preparation of CNCs and NaSCNCs

Medical absorbent cotton was dispersed in 64% sulfuric acid and the proportion of the cotton to acid was 1:8.75 (g/mL) (Dong et al., 1998). This suspension was kept at 45°C for 45 min, and then an equal part of distilled water was added. After that, the suspension was centrifuged at 10000 r/min for 10 min to remove excess acid and water. The precipitate was then dialyzed with distilled water for 7 days until the effluent remained at neutral pH. Finally, CNCs were recovered by freeze-drying from the water dispersions.

Freeze-dried CNCs (3 g) were mixed with succinic anhydride (15 g) and then reacted at 120°C for 12 hr under pyridine (30 mL) reflux. After the reaction, the unreacted succinic anhydride was removed by washing with distilled water, ethanol and acetone several times and the product was dried in vacuum at 60°C. Finally, SCNCs were obtained.

NaSCNCs were prepared by treatment of SCNCs with saturated sodium bicarbonate solution for 2 hr under constant stirring at room temperature followed by filtration. The product was washed with distilled water and acetone. Finally, the NaSCNCs were dried in vacuum at 60°C.

1.3 Carboxylic content and the mass gain percent

The carboxylic content of SCNCs was determined by the back titration method (Liu et al., 2010). Sample of 0.1 g was treated with 100 mL 0.01 mol/L NaOH standard solution by stirring at room temperature for 1 hr. Several drops of phenolphthalein indicator were added. The above solution was back-titrated against 0.01 mol/L standard HCl solution until the solution turned from the pale pink to colorless. The carboxylic content of SCNCs (C_{COOH} , mmol/g) was calculated by Eq. (1):

$$C_{\text{COOH}} = \frac{V_{\text{NaOH}} \times C_{\text{NaOH}} - V_{\text{HCl}} \times C_{\text{HCl}}}{m} \quad (1)$$

where, V_{NaOH} (mL) and V_{HCl} (mL) are the volume of standard NaOH used and standard HCl consumed, respectively, C_{NaOH} (mol/L) and C_{HCl} (mol/L) are the molarity of standard NaOH and HCl, respectively, and m (g) is the weight of the analyzed sample.

1.4 Characterization of materials

Fourier transform infrared spectrometer (FT-IR) (6700, Thermo Nicolet, USA) and a solid-state CP/MAS ^{13}C nuclear magnetic resonance (NMR) spectrometer (Bruker Avance III 400, Bruker, Germany) were used to verify the presence of functional groups in the adsorbent. The

morphology of the samples was observed with a S-4300 scanning electron microscope (Hitachi, Japan) operating at 15 kV. Transmission electron microscopy was conducted using a JEM-1011 instrument (JEOL, Japan). X-ray photoelectron spectroscopy (XPS) data were obtained with an ESCALab220i-XL electron spectrometer (VG Scientific, USA) using 300W AlK α radiation. The zeta potential was measured with a Zetasizer (Nano-ZS, Malvern Instruments, England).

1.5 Adsorption of heavy metal ions

The adsorption experiments were performed on a platform shaker at 200 r/min and $(25 \pm 2)^\circ\text{C}$ using 150 mL shaker flasks. The effects of contact time, pH, initial adsorption concentration, coexisting ions and the regeneration performance were investigated. In order to avoid the formation of insoluble metal hydroxides, the pH of adsorption kinetics experiments was kept at 6.0 for Cd $^{2+}$ and 5.5 for Pb $^{2+}$ (Gurgel and Gil, 2009). Either 0.1 mol/L HCl or 0.1 mol/L NaOH solution was used to adjust the pH values during the adsorption experiments. The metal ion concentration was analyzed using an inductively coupled plasma optical emission spectrometer (ICP-OES, Optima 2000, Perkin Elmer, USA). The adsorption capacity q_e (mg/g) was calculated as described by Eq. (2):

$$q_e = \frac{(C_0 - C_e)V}{m} \quad (2)$$

where, C_0 (mg/L) is the initial metal ion concentration, C_e (mg/L) is the metal ion equilibrium concentration, V (L) is the volume of the metal ion solution and m (g) is the mass of adsorbent. The adsorbent dose was kept at 1 g/L for all the adsorption experiments.

2 Results and discussion

2.1 Characterization of SCNCs and NaSCNCs

The esterification of CNCs was confirmed by the FT-IR spectra. **Figure 1A** shows the FT-IR spectra of cotton, CNCs and SCNCs. In the spectra of cotton and CNCs

(**Fig. 1A line a and line b**), the spectra exhibit typical peaks for many functional groups of cellulose. The broad band at 3338 cm^{-1} is attributed to the presence of free and hydrogen bonded OH stretching vibration and the other one at 670 cm^{-1} is attributed to the OH out-of-plane bending vibration. The band at 2900 cm^{-1} is due to the C–H asymmetric and symmetric tensile vibration. Bands corresponding to C–H bending vibrations were observed at 1280 and 1337 cm^{-1} . The peak at 1636 cm^{-1} originates from the bending mode of the absorbed water. The strong absorption at 1056 cm^{-1} relates to C–O and C–O–C stretching vibrations, and the 1160 cm^{-1} peak relates to the C–O antisymmetric bridge stretching vibration. The peak at 1429 cm^{-1} corresponds to the CH $_2$ bending vibration. An absorption band at 898 cm^{-1} arises from the β -glycosidic linkages. These absorption bands are all characteristic absorption bands of cellulose, indicating that the structure of the CNCs was not destroyed by sulfuric acid hydrolysis. There are two peaks at 1735 and 1718 cm^{-1} in the spectrum of SCNCs (**Fig. 1A line c**), indicating the presence of two carbonyl groups. The peak at 1735 cm^{-1} is due to the carbonyl group of the ester and the peak at 1718 cm^{-1} is assigned to the carbonyl group of carboxylic acid. As expected, the absence of any absorption band at 1850 and 1780 cm^{-1} confirms the product to be free of non-reacted succinic anhydride (Liu et al., 2010). Thus, it is demonstrated that the CNCs were successfully modified with succinic anhydride.

The NMR spectra of CNCs and SCNCs are shown in **Fig. 1B**. In the spectrum of CNCs (**Fig. 1B line b**), all signals, i.e. those at 104.7 ppm (C-1), 89.8 ppm (C-4 of crystalline cellulose), 74.7 ppm (C-5), 72 ppm (C-2 and C-3), and 69.5 ppm (C-6 of crystalline cellulose) (Liu et al., 2010), are attributed to six carbon atoms of the glucose unit. However, there is no signal of C-4 and C-6 of amorphous cellulose in the spectrum, suggesting the complete disruption of the cellulose amorphous structure during the acid hydrolysis of cotton. Notably, two more intense signals appear in the spectrum of SCNCs (**Fig. 1B line c**) in addition to those of CNCs, due to carbon atoms of carboxylic groups (C-7 and C-10) at 173.8 ppm and

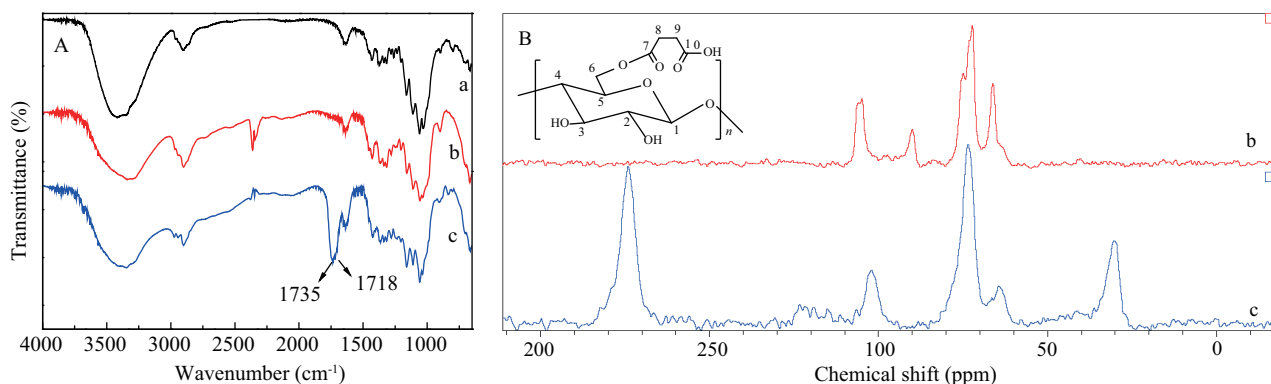


Fig. 1 FT-IR spectra (A) and solid-state CP/MAS ^{13}C NMR spectra (B) of cotton (line a), CNCs (line b) and SCNCs (line c).

methylene groups (C-8 and C-9) at 30.1 ppm. The presence of these two intense signals proves that the esterification did occur, and according to Eq. (1), the carboxylic content of the SCNCs was 4.91 mmol/g.

CNCs dispersed in water present individual rodlike particles, about 30 nm in diameter and several hundred nanometers in length (Fig. 2d). However, after drying, a serious agglomeration occurs due to their large specific surface area and leads to the formation of giant particles, and the surface of these particles looks irregular and smooth, as shown in Fig. 2a. Clearly, the sizes of the SCNCs particles are smaller than those of CNCs and the surface appears to have a few cracks (Fig. 2b). Figure 2c shows that the cracks of NaSCNCs further expand after drying. These results demonstrate that the surface hydroxyl groups reacted with succinic anhydride, leading to the slight destruction of the aggregates.

2.2 Adsorption kinetics

Contact time is an important factor in evaluating the adsorption efficiency, which helps to determine the rate of maximum removal of solutes. The effect of contact time on Pb^{2+} , Cd^{2+} ions adsorption in aqueous solution is presented in Fig. 3a and b. The adsorption rates of Pb^{2+} and Cd^{2+} ions on SCNCs, NaSCNCs, and CNCs were very fast. Especially for NaSCNCs, the adsorption equilibrium was reached within 5 min, and the equilibrium time of SCNCs was 120 and 150 min for Pb^{2+} and Cd^{2+} , respectively. Although the adsorption equilibrium process

of CNCs was also rapid, the adsorption capacity was quite low compared with those of SCNCs and NaSCNCs. This fact indicates that modification of cellulose nanocrystals with succinic anhydride improves adsorption performance.

In order to understand the adsorption process, various kinetic models such as the pseudo first-order kinetics model, pseudo second-order kinetics model and intraparticle diffusion kinetics model are used to study the adsorption type and mechanism. It has been found that the pseudo second-order kinetic model fits the experimental data best in most cases. Therefore, the pseudo-second-order kinetic model was used to study the adsorption process in the present work.

The pseudo second-order kinetic model (Ho and McKay, 1999; Ho et al., 2000) is described as:

$$q_t = \frac{kq_e^2 t}{1 + kq_e t} \quad (3)$$

$$\frac{t}{q_t} = \frac{1}{kq_e^2} + \frac{1}{q_e} t \quad (4)$$

where, q_t (mg/g) and q_e (mg/g) are the amount of metal adsorbed at time t and at equilibrium, respectively, and k is the rate constant $\text{g}/(\text{mg} \cdot \text{min})$.

When $t \rightarrow 0$, the initial adsorption rate h can be defined as follows:

$$h = kq_e^2 \quad (5)$$

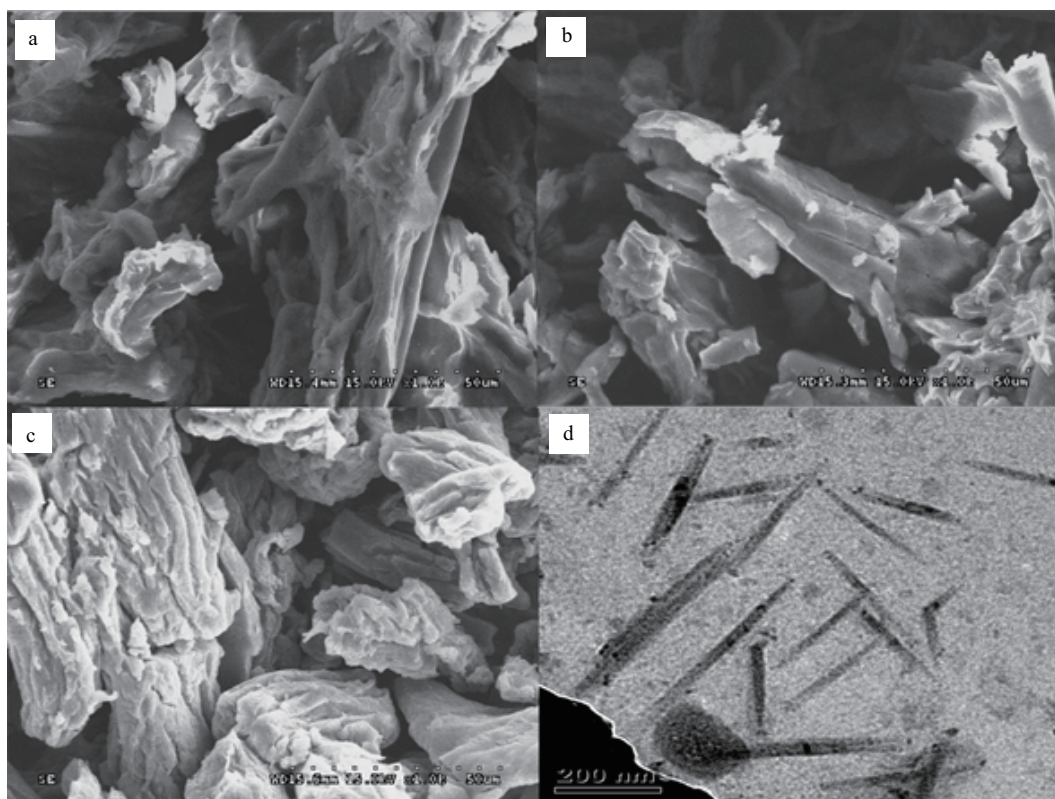


Fig. 2 SEM images of CNCs (a), SCNCs (b), NaSCNCs (c) and TEM image of CNCs (d).

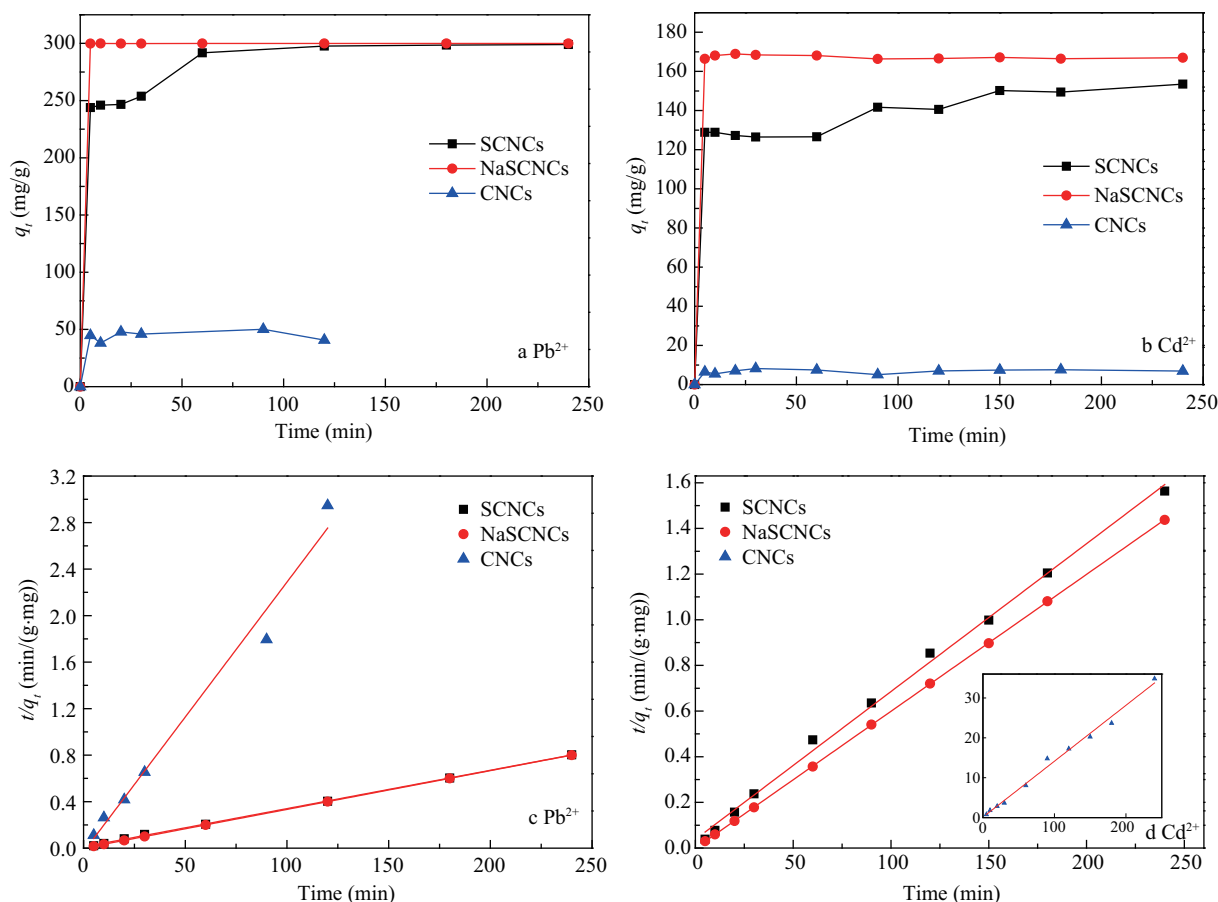


Fig. 3 Effect of contact time on Pb^{2+} (a) and Cd^{2+} (b) adsorption and pseudo second-order adsorption kinetic plot for Pb^{2+} (c) and Cd^{2+} (d) adsorption. Initial concentration: 300 mg/L for Pb^{2+} , 200 mg/L for Cd^{2+} .

The kinetic parameters were calculated from the slope and intercept of the plot of t/q_t vs. t by linear regression analysis (Fig. 3c and d) and the results are presented in Table 1. It can be seen that the experimental data can be well described by the pseudo second-order equation considering the good correlation coefficient ($R^2 > 0.99$), and the values of $q_{e(\text{theo})}$ obtained from pseudo second-order kinetic model agree perfectly with the experimental $q_{e(\text{exp})}$ values. Therefore, it is concluded that the adsorption process can be well explained by the pseudo second-order kinetic model and the process may be a chemical adsorption process through sharing or exchange of electrons between adsorbent and adsorbate (Bulut and Tez, 2007). In addition, it is noted that the initial adsorption rate of NaSCNCs was faster than that of SCNCs and CNCs. This

can be explained by its different adsorption mechanism.

2.3 Effect of pH

One important factor in metal ion removal from aqueous solutions is the pH, which can affect the adsorbent surface charge and the degree of ionization. Figure 4 shows the effect of pH on the adsorption behavior. It was found that the adsorption capacities of Pb^{2+} and Cd^{2+} on SCNCs and NaSCNCs increased with increasing pH. When the pH values are lower ($\text{pH} < \text{pH}_{\text{PZC}} = 1.25$), the concentration of protons competing with metal ions for the active sites is higher. Meanwhile, the adsorbent surface is positively charged and metal ions with positive charge have difficulty approaching the functional groups due to electrostatic repulsion. Thus adsorption capacities were found to be

Table 1 Kinetic parameters of pseudo-second-order model for Pb^{2+} , Cd^{2+} adsorption

Metal ion	Adsorbents	$q_{e(\text{theo})}$ (mg/g)	$q_{e(\text{exp})}$ (mg/g)	k_2 (g/(mg·min))	h (g/(mg·min))	R^2
Pb^{2+}	CNCs	43.1	50.2	1.62×10^{-2}	30.73	0.99462
	SCNCs	303	299.7	0.1×10^{-2}	96.62	0.99967
	NaSCNCs	300.3	299.9	52×10^{-2}	46893.65	1
Cd^{2+}	CNCs	7.1	7.4	18.64×10^{-2}	9.48	0.99050
	SCNCs	154.32	150.22	0.111×10^{-2}	26.34	0.99694
	NaCNCs	166.66	166.50	4.17×10^{-2}	1216.31	0.99999

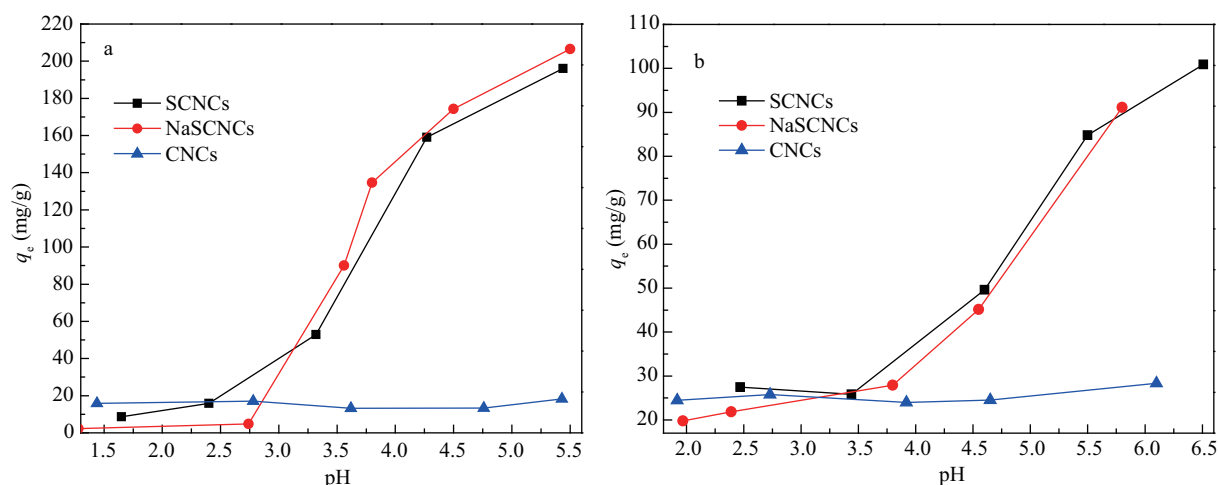


Fig. 4 Effect of pH on Pb^{2+} (a) and Cd^{2+} (b). Initial concentration: 300 mg/L for Pb^{2+} , 200 mg/L for Cd^{2+} .

low at lower pH values. With the increase of pH ($\text{pH} > \text{pH}_{\text{PZC}} = 1.25$), the concentration of protons decreases and the adsorbent surface charge becomes negative. Therefore, the electrostatic attraction increases between the metal ions and the adsorbent, which leads to a higher adsorption capacity. However, it was found that the adsorption capacity of CNCs was not affected by pH. This is mainly due to the fact that CNCs bear numerous hydroxyl groups and a little residual sulphate groups. In the studied pH range, the sulphate groups, which remained fully ionized, as well as the hydroxyl groups, are less affected by the pH. The optimum pH values which correspond to the maximum adsorption capacity of Pb^{2+} and Cd^{2+} were observed at 5.5 and 6.5, respectively. The results are consistent with the report of Gurgel and Gil (2009).

2.4 Adsorption isotherms

Adsorption isotherms are often used to describe the relationship between the adsorbent and adsorbate. The Langmuir isotherm model is the most widely used sorption isotherm for the removal of metal ions from aqueous solution. This model is based on the assumption that the adsorbate forms a saturated molecular layer (monolayer) on the adsorbent surface, that the surface sites have the same energy, and that there is no solute-solute or solute-solvent interaction in either phase or transmigration of adsorbate on the plane of the surface (Bulut and Tez, 2007; Davis et al., 2003; Gurgel and Gil, 2009; Langmuir, 1918). The general form of the Langmuir isotherm model can be expressed as:

$$q_e = \frac{Q_{\max} b C_e}{1 + b C_e} \quad (6)$$

The linearized form of the Langmuir isotherm model can be expressed as:

$$\frac{C_e}{q_e} = \frac{1}{b Q_{\max}} + \frac{C_e}{Q_{\max}} \quad (7)$$

where, C_e (mg/L) is the equilibrium concentration of metal

ions in solution, q_e (mg/g) is the equilibrium adsorption capacity at this solution concentration, Q_{\max} (mg/g) is the maximum adsorption capacity per gram of sorbent, and b (L/mg) is the Langmuir constant related to the energy of adsorption. The Langmuir parameters were calculated from the slope and intercept of different straight lines. The results are listed in Table 2.

The high correlation coefficients ($R^2 > 0.97$) indicate that the experimental data can be well fitted by the Langmuir model and this model can well explain the adsorption process of Pb^{2+} and Cd^{2+} on CNCs, SCNCs and NaSCNCs. The Langmuir parameter Q_{\max} reflects the theoretical maximum adsorption capacity of an adsorbent. From the values of Q_{\max} in Table 2, the maximum adsorption capacities of SCNCs, NaSCNCs and CNCs for Pb^{2+} and Cd^{2+} varied in the order NaSCNCs > SCNCs > CNC. This is a remarkable improvement compared to Q_{\max} of CNCs and demonstrates that an excellent adsorbent was obtained. Comparison of Q_{\max} and $Q_{\max(\text{exp})}$ showed that the two values were very consistent, indicating that the adsorption was a monolayer adsorption process. In addition, the Q_{\max} of NaSCNCs was higher than that of SCNCs. This could be explained by the different adsorption mechanisms. Thus, when materials with carboxyl acid groups are applied in the removal of heavy metal, it is essential to turn the carboxyl acid group into carboxylate. The Langmuir parameter b indicates the adsorption bond energy between adsorbent and metal ion. A strong bond energy between active sites and metal ions leads to a high adsorption capacity. It was found that modified CNCs exhibited a larger bond energy than unmodified CNCs, which was consistent with the observed adsorption capacity.

The dimensionless constant separation factor for equilibrium parameter (R_L) (Deniz and Saygideger, 2010) can be defined as:

$$R_L = \frac{1}{1 + b C_0} \quad (8)$$

where, C_0 (mg/L) is the initial concentration of metal ion

Table 2 Langmuir parameters for Pb²⁺ and Cd²⁺ adsorption

Metal ion	Adsorbents	Q_{\max} (mg/g)	$Q_{\max(\text{exp})}$ (mg/g)	b (L/mg)	R^2
Pb ²⁺	CNCs	27.9	25	0.04	0.97285
	SCNCS	367.6	365.9	1.81	0.99807
	NaSCNCs	465.1	458.3	4.13	0.99962
Cd ²⁺	CNCs	1.9	2	0.09	0.99592
	SCNCS	259.7	256.3	2.29	0.99826
	NaSCNCs	344.8	335	41.88	0.99994

and b (L/mg) is the Langmuir constant. The value of R_L indicates whether the type of isotherm is irreversible ($R_L = 0$), favorable ($0 < R_L < 1$), linear ($R_L = 1$) or unfavorable ($R_L > 1$). In this study, the values of R_L vary between 0 and 1, indicating that the adsorption process is favorable.

2.5 Adsorption mechanism

Figure 5 shows the FT-IR spectra of SCNCs, NaSCNCs, lead-loaded SCNCs and cadmium-loaded SCNCs from 2000 to 1100 cm⁻¹. The band at 1735 cm⁻¹ corresponding to the ester carbonyl double bond did not change after the sorption of metal ions onto the SCNCs. However, the free carbonyl double bond stretching band at 1718 cm⁻¹ exhibited an evident shift to a lower frequency at 1575, 1548 and 1540 cm⁻¹ for NaSCNCs, cadmium-loaded SCNCs and lead-loaded SCNCs, respectively, while the carboxyl C–O bond shifted from 1205 to around 1415 cm⁻¹. These shifts demonstrate the complexation of carbonyl groups by dative coordination (Fourrest and Volesky, 1996). The distance between C=O and C–O bands ($\Delta = \nu_{\text{C=O}} - \nu_{\text{C–O}}$) is related to the relative symmetry of the carboxyl group and reflects the nature of the coordination status. Fuks et al. (2006) reported that monodentate complexes presented the highest Δ ($\Delta_{\text{complex}} \gg \Delta_{\text{Nasalt}}$); bidentate chelating complexes exhibited the lowest Δ ($\Delta_{\text{complex}} \ll \Delta_{\text{Nasalt}}$); while bidentate bridging complexes displayed intermediate Δ ($\Delta_{\text{complex}} \leq \Delta_{\text{Nasalt}}$). The distances for NaSCNCs, cadmium-loaded SCNCs and lead-loaded SCNCs were 157, 132

and 128 cm⁻¹ respectively. These results demonstrate that cadmium or lead binding with the carboxyl groups formed a bidentate bridging or bidentate chelating structure, rather than a monodentate structure. Additionally, the Δ change indicates more involvement of carboxyl groups forming complexes with metal ions (Liu et al., 2011a).

XPS analysis of the adsorbents before and after metal ion sorption was conducted to study the interaction between the functional groups and the adsorbed metal ions. The wide scan XPS spectra of SCNCs (**Fig. 6A**) and NaSCNCs (**Fig. 6B**) showed that peaks at 138.5 and 405.3 eV appeared after the adsorption of Pb²⁺ and Cd²⁺, respectively. These indicate that the Pb²⁺ and Cd²⁺ accumulated on the surface of the adsorbents. Moreover, for NaSCNCs, the peak at 1071.2 eV for Na 1s disappeared after the Pb²⁺ and Cd²⁺ ion adsorption, which is attributed to the ion exchange of sodium ions by Pb²⁺ and Cd²⁺ ions (Zheng et al., 2009).

High resolution spectra of C 1s and O 1s regions are shown in **Fig. 7**. The C 1s spectrum of SCNCs presents four peaks with BE of 284.7, 286.2, 287.9, 288.7 eV, resolved via deconvolution (**Fig. 7a**). These peaks can be assigned to C atoms in the form of C–C, C–O (alcoholic or ether), O–C–O (ether) and O–C=O (carboxylate groups), respectively (Chen et al., 2002a; Lim et al., 2008; Liu et al., 2011a). After Pb²⁺ and Cd²⁺ adsorption onto the SCNCs, the binding energy of C–O, O–C–O and O–C=O shifted to 286.4, 288.2 and 288.9 eV, respectively (**Fig. 7b** and **c**). This demonstrates that ether and carboxylate groups in the SCNCs were involved in the metal ion adsorption. Additionally, the O–C=O peak at 288.7 eV dramatically decreased, indicating that carboxyl-metal complexes were formed between unoccupied electron orbitals of bivalent metal ions and lone pair electrons of oxygen atoms of carboxylate groups, thus decreasing the electron density at the adjacent carbon atom in C=O and C–O (Chen and Yang, 2006; Liu et al., 2011b). The O 1s peaks of SCNCs can be deconvoluted into three individual component peaks (**Fig. 7d**), which are attributed to C=O (531.4 eV), C–O (532.2 eV) and COO⁻ (533.3 eV). The peaks after Pb²⁺ and Cd²⁺ adsorption had a certain degree of shift (**Fig. 7e** and **f**), which is due to the binding of Pb²⁺ and Cd²⁺ ions onto the oxygen atoms, and thus reducing its electron density (Lim et al., 2008). The changes in the binding energy indicate that C=O, C–O and COO⁻ are involved in the adsorption of Pb²⁺ and Cd²⁺.

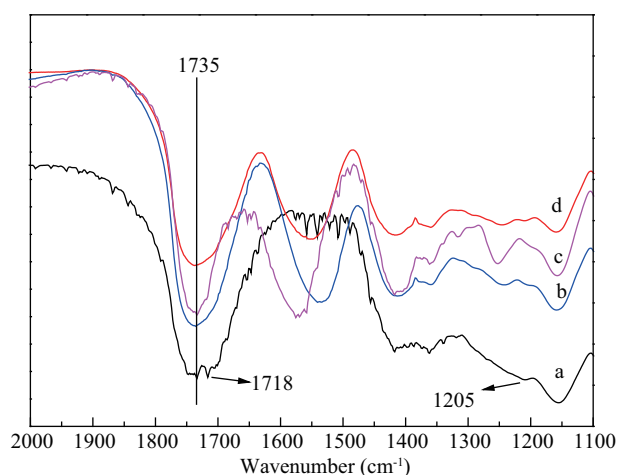


Fig. 5 FT-IR spectra of SCNCs (line a), lead-loaded SCNCs (line b), NaSCNCs (line c) and cadmium-loaded SCNCs (line d) from 2000 to 1100 cm⁻¹.

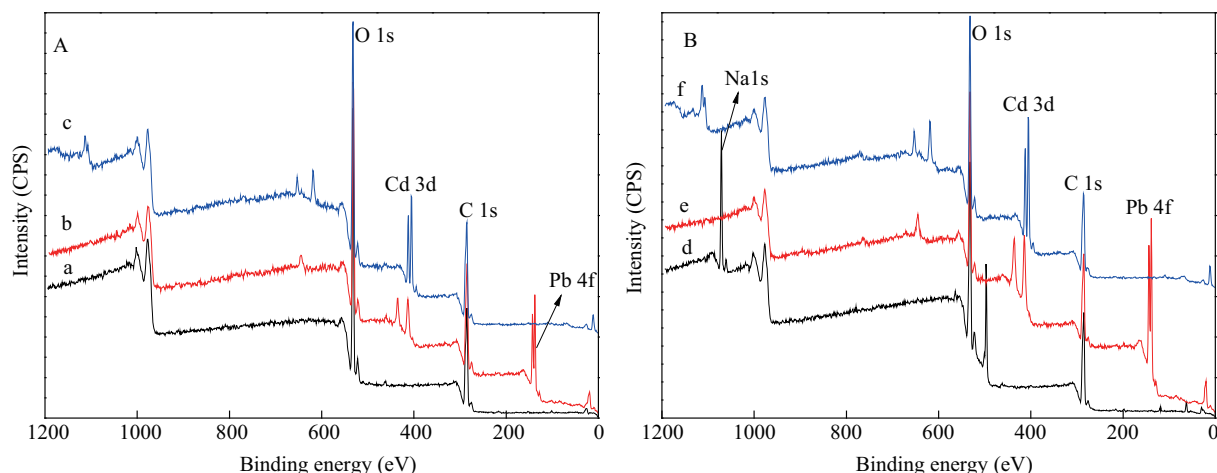


Fig. 6 Wide scan XPS spectra of adsorbents SCNCs (A) and NaSCNCs (B). line a: SCNCs; line b: lead-loaded SCNCs; line c: cadmium-loaded SCNCs; line d: NaSCNCs; line e: lead-loaded NaSCNCs; line f: cadmium-loaded NaSCNCs.

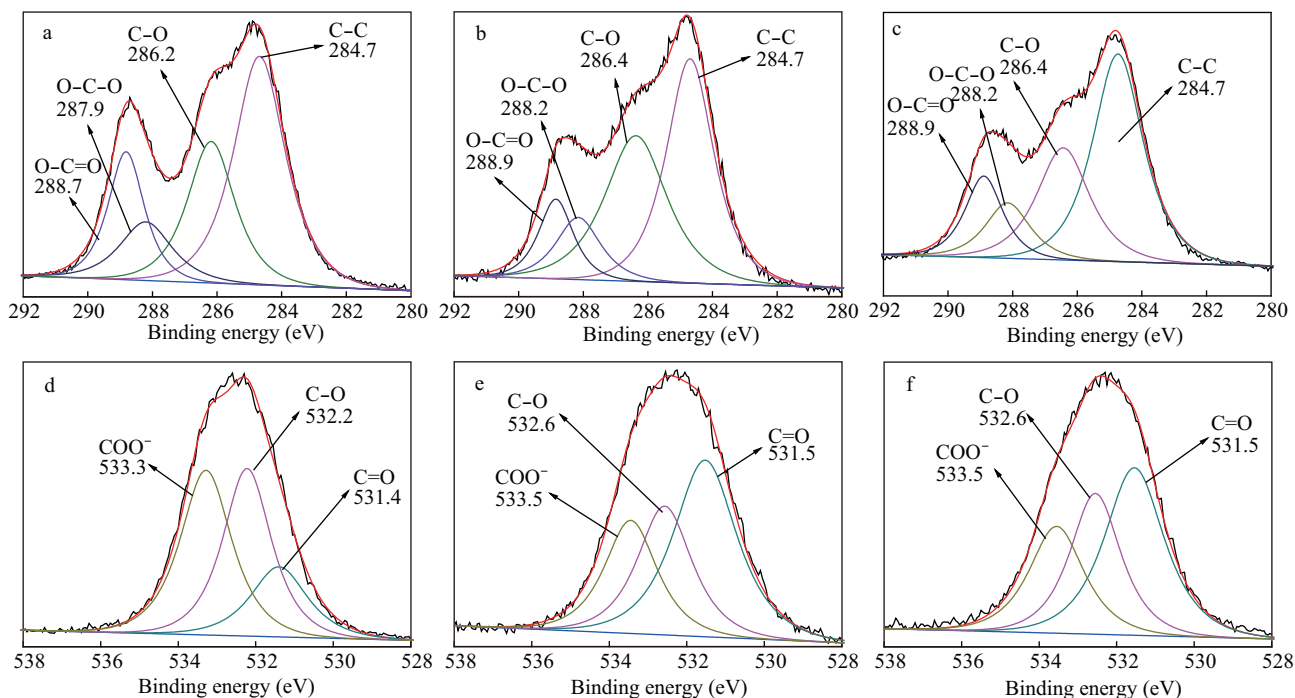


Fig. 7 XPS spectra of adsorbent: (a) C 1s of SCNCs; (b) C 1s of lead-loaded SCNCs; (c) C 1s of cadmium-loaded SCNCs; (d) O 1s of SCNCs; (e) O 1s of lead-loaded SCNCs; (f) O 1s of cadmium-loaded SCNCs.

2.6 Effect of coexisting ions on Pb^{2+} and Cd^{2+} adsorption

The effect of coexisting ions on Pb^{2+} and Cd^{2+} adsorption were studied by adding other ions, such as Ca^{2+} , Mg^{2+} and K^{+} . **Figure 8** shows the simultaneous adsorption of Pb^{2+} and Cd^{2+} without and with coexisting ions. It can be seen that the removal rate of Pb^{2+} was much higher than Cd^{2+} without coexisting ions. In conclusion, the two adsorbents were able to selectively adsorb Pb^{2+} from aqueous solution. Meanwhile, the adsorption capacity of Cd^{2+} on NaSCNCs was higher than that on SCNCs.

For the simultaneous adsorption of Pb^{2+} and Cd^{2+} with coexistent ions, the effect of coexisting ions on Pb^{2+}

adsorption was very small compared with the adsorption without coexisting ions. However, the removal rate of Cd^{2+} decreased more than that for adsorption without coexisting ions. This means that the binding of Pb^{2+} was relatively unaffected by other metals (Taty-Costodes et al., 2003) and the adsorbents have quite good selectivity for Pb^{2+} , which is due to the different ionic radius of Pb^{2+} and Cd^{2+} (Low et al., 2000). Although a larger ionic radius reduces the electrostatic nature of a metal ion, it favors interactions of a covalent nature between metal ions and the functional groups of an adsorbent (Lau et al., 1999; Low et al., 2004). Therefore, the adsorption of Pb^{2+} with larger ionic radius is relatively unaffected and the adsorption of Pb^{2+} is more favorable than that of Cd^{2+} . In addition, the adsorption of

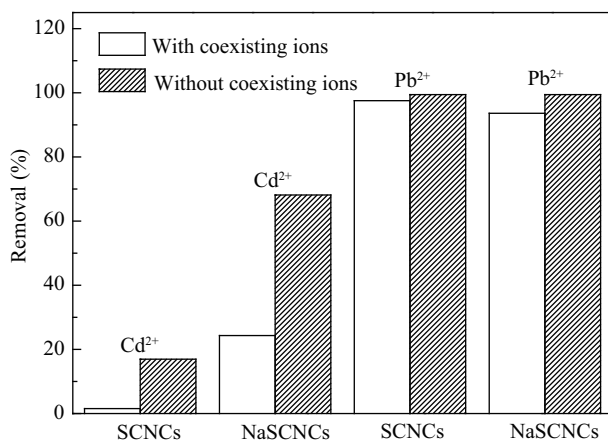


Fig. 8 Simultaneous adsorption of Pb^{2+} and Cd^{2+} with and without coexisting ions. Pb^{2+} , 300 mg/L; Cd^{2+} , 300 mg/L; Ca^{2+} , 100 mg/L; Mg^{2+} , 100 mg/L; K^+ , 100 mg/L.

Pb^{2+} and Cd^{2+} on NaSCNCs is better than that on SCNCs, especially for the removal of Cd^{2+} .

2.7 Regeneration of adsorbent

In practical application, it is very important to investigate the ability of an adsorbent to be regenerated and reused. As shown in **Fig. 9**, the adsorption capacities of Pb^{2+} and Cd^{2+} on SCNCs decreased when SCNCs were regenerated using HCl solution. Due to the abundant hydrogen ions in the solution, a dominant protonation reaction takes place between hydrogen ions and active sites (COO^- groups) (Ren et al., 2012). Thus, the complexation between the active sites and metal ions is destroyed and the adsorbent is regenerated. However, the structure of cellulose and its adsorption active sites are easily destroyed by the acid solution, leading to lower adsorption capacities after each regeneration cycle. When lead or cadmium-loaded NaSCNCs are added into a saturated NaCl solution, the metal ions adsorbed by NaSCNCs are surrounded by the numerous sodium ions and are replaced continuously by sodium ions through ion exchange. Additionally, the saturated NaCl solution is a mild desorption solution which

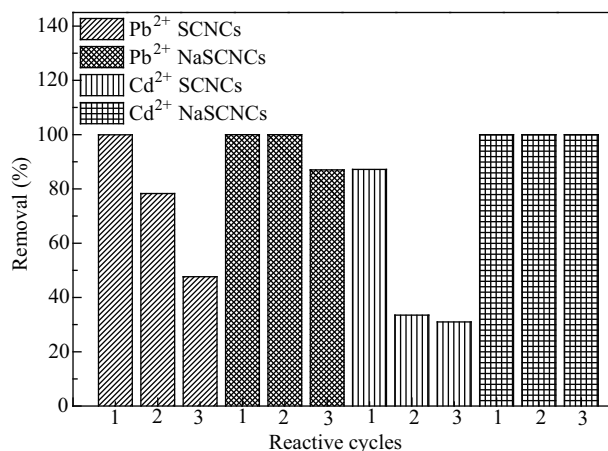


Fig. 9 Regeneration efficiency of SCNCs and NaSCNCs.

does not destroy the active sites. Therefore, the adsorption on NaSCNCs remained at a high value after two recycling procedures.

3 Conclusions

SCNCs were synthesized by CNCs with succinic anhydride and then further treated with saturated NaHCO_3 aqueous solution to obtain NaSCNCs. Both SCNCs and NaSCNCs could be used for the removal of heavy metal ions from water. The results of adsorption experiments demonstrated that the adsorption rates of Pb^{2+} and Cd^{2+} ions on SCNCs and NaSCNCs were very fast, especially on NaSCNCs. The adsorption capacities of Pb^{2+} and Cd^{2+} on SCNCs and NaSCNCs depended strongly upon the pH of the solution and increased with increasing pH. NaSCNCs exhibited a higher adsorption capacity for Pb^{2+} and Cd^{2+} ions than SCNCs. Moreover, the adsorbents had high selectivity for Pb^{2+} and the adsorption of Cd^{2+} on NaSCNCs with coexisting ions was better than that on SCNCs. NaSCNCs were easily regenerated with mild saturated NaCl. The mechanism studies confirmed that the adsorption process of heavy metal ions on SCNCs was a complexation process, while ion-exchange was the principal mechanism for the removal of heavy metal ions from NaSCNCs. Due to the ion-exchange mechanism, NaSCNCs exhibited more excellent properties than SCNCs. Therefore, it was essential to convert the carboxyl groups into carboxylates for this adsorbent containing carboxyl groups.

Acknowledgments

This work was supported by the National Basic Research Program (973) of China (No. 2011CB933700) of Ministry of Science and Technology of China.

References

- Anirudhan T S, Sreekumari S S, 2011. Adsorptive removal of heavy metal ions from industrial effluents using activated carbon derived from waste coconut buttons. *Journal of Environmental Sciences*, 23(12): 1989–1998.
- Belhafaoui B, Aziz A, Elandaloussi E, Ouali M S, De Menorval L C, 2009. Succinate-bonded cellulose: A regenerable and powerful sorbent for cadmium-removal from spiked high-hardness groundwater. *Journal of Hazardous Materials*, 169(1-3): 831–837.
- Bulut Y, Tez Z, 2007. Adsorption studies on ground shells of hazelnut and almond. *Journal of Hazardous Materials*, 149(1): 35–41.
- Canet L, Ilpide M, Seta P, 2002. Efficient facilitated transport of lead, cadmium, zinc, and silver across a flat-sheet-supported liquid membrane mediated by lasalocid A. *Separation Science and Technology*, 37(8): 1851–1860.
- Chen J P, Hong L A, Wu S N, Wang L, 2002a. Elucidation of interactions between metal ions and Ca alginate-based ion-exchange resin by spectroscopic analysis and modeling

- simulation. *Langmuir*, 18(24): 9413–9421.
- Chen J P, Yang L, 2006. Study of a heavy metal biosorption onto raw and chemically modified *Sargassum* sp. via spectroscopic and modeling analysis. *Langmuir*, 22(21): 8906–8914.
- Chen X M, Chen G H, Yue P L, 2002b. Novel electrode system for electroflotation of wastewater. *Environmental Science & Technology*, 36(4): 778–783.
- da Silva Filho E C, de Melo J C P, da Fonseca M G, Airoidi C, 2009. Cation removal using cellulose chemically modified by a Schiff base procedure applying green principles. *Journal of Colloid and Interface Science*, 340(1): 8–15.
- Davis T A, Volesky B, Mucci A, 2003. A review of the biochemistry of heavy metal biosorption by brown algae. *Water Research*, 37(18): 4311–4330.
- Deniz F, Saygideger S D, 2010. Equilibrium, kinetic and thermodynamic studies of Acid Orange 52 dye biosorption by *Paulownia tomentosa* Steud. leaf powder as a low-cost natural biosorbent. *Bioresource Technology*, 101(14): 5137–5143.
- Dong X M, Revol J F, Gray D G, 1998. Effect of microcrystallite preparation conditions on the formation of colloid crystals of cellulose. *Cellulose*, 5(1): 19–32.
- Esalah J O, Weber M E, Vera J H, 2000. Removal of lead, cadmium and zinc from aqueous solutions by precipitation with sodium di-(*n*-octyl) phosphinate. *Canadian Journal of Chemical Engineering*, 78(5): 948–954.
- Fourest E, Volesky B, 1996. Contribution of sulfonate groups and alginate to heavy metal biosorption by the dry biomass of *Sargassum fluitans*. *Environmental Science & Technology*, 30(1): 277–282.
- Friberg L T, 1985. The rationale of biological monitoring of chemicals with special reference metals. *American Industrial Hygiene Association Journal*, 46(11): 633–642.
- Fuks L, Filipiuk D, Majdan M, 2006. Transition metal complexes with alginate biosorbent. *Journal of Molecular Structure*, 792–793: 104–109.
- Güçlü G, Gürda G, Özgümü S, 2003. Competitive removal of heavy metal ions by cellulose graft copolymers. *Journal of Applied Polymer Science*, 90(8): 2034–2039.
- Gurgel L V A, Gil L F, 2009. Adsorption of Cu(II), Cd(II) and Pb(II) from aqueous single metal solutions by succinylated twice-mercerized sugarcane bagasse functionalized with triethylenetetramine. *Water Research*, 43(18): 4479–4488.
- Hasani M, Cranston E D, Westman G, Gray D G, 2008. Cationic surface functionalization of cellulose nanocrystals. *Soft Matter*, 4(11): 2238–2244.
- Ho Y S, McKay G, 1999. Pseudo-second order model for sorption processes. *Process Biochemistry*, 34(5): 451–465.
- Ho Y S, Ng J C Y, McKay G, 2000. Kinetics of pollutant sorption by biosorbents: Review. *Separation and Purification Methods*, 29(2): 189–232.
- Karnitz O Jr, Gurgel L V A, de Melo J C P, Botaro V R, Melo T M S, de Freitas Gil R P et al., 2007. Adsorption of heavy metal ion from aqueous single metal solution by chemically modified sugarcane bagasse. *Bioresource Technology*, 98(6): 1291–1297.
- Karnitz O, Gurgel L V A, Gil L F, 2010. Removal of Ca(II) and Mg(II) from aqueous single metal solutions by mercerized cellulose and mercerized sugarcane bagasse grafted with EDTA dianhydride (EDTAD). *Carbohydrate Polymers*, 79(1): 184–191.
- Kloser E, Gray D G, 2010. Surface grafting of cellulose nanocrystals with poly(ethylene oxide) in aqueous media. *Langmuir*, 26(16): 13450–13456.
- Langmuir I, 1918. The adsorption of gases on plane surfaces of glass, mica and platinum. *Journal of the American Chemical Society*, 40(9): 1361–1403.
- Lau P S, Lee H Y, Tsang C C K, Tam N F Y, Wong Y S, 1999. Effect of metal interference, pH and temperature on Cu and Ni biosorption by *Chlorella vulgaris* and *Chlorella miniata*. *Environmental Technology*, 20(9): 953–961.
- Li L X, Dong J H, Nenoff T M, 2007. Transport of water and alkali metal ions through MFI zeolite membranes during reverse osmosis. *Separation and Purification Technology*, 53(1): 42–48.
- Li Q Z, Chai L Y, Wang Q W, Yang Z H, Yan H X, Wang Y Y, 2010. Fast esterification of spent grain for enhanced heavy metal ions adsorption. *Bioresource Technology*, 101(10): 3796–3799.
- Lim S F, Zheng Y M, Zou S W, Chen J P, 2008. Characterization of copper adsorption onto an alginate encapsulated magnetic sorbent by a combined FT-IR, XPS and mathematical modeling study. *Environmental Science & Technology*, 42(7): 2551–2556.
- Liu C F, Zhang A P, Li W Y, Yue F X, Sun R C, 2010. Succinylation of cellulose catalyzed with iodine in ionic liquid. *Industrial Crops and Products*, 31(2): 363–369.
- Liu H J, Yang F, Zheng Y M, Kang J, Qu J H, Chen J P, 2011a. Improvement of metal adsorption onto chitosan/*Sargassum* sp. composite sorbent by an innovative ion-imprint technology. *Water Research*, 45(1): 145–154.
- Liu W J, Zeng F X, Jiang H, Yu H Q, 2011b. pH-dependent interactions between lead and *Typha angustifolia* biomass in the biosorption process. *Industrial & Engineering Chemistry Research*, 50(10): 5920–5926.
- Low K S, Lee C K, Liew S C, 2000. Sorption of cadmium and lead from aqueous solutions by spent grain. *Process Biochemistry*, 36(1-2): 59–64.
- Low K S, Lee C K, Mak S M, 2004. Sorption of copper and lead by citric acid modified wood. *Wood Science and Technology*, 38(8): 629–640.
- Lu L L, Chen L H, Shao W J, Luo F, 2010. Equilibrium and kinetic modeling of Pb(II) biosorption by a chemically modified orange peel containing cyanex 272. *Journal of Chemical and Engineering Data*, 55(10): 4147–4153.
- Ma L, Xu R K, Jiang J, 2010. Adsorption and desorption of Cu(II) and Pb(II) in paddy soils cultivated for various years in the subtropical China. *Journal of Environmental Sciences*, 22(5): 689–695.
- Musyoka S M, Ngila J C, Moodley B, Petrik L, Kindness A, 2011. Synthesis, characterization, and adsorption kinetic studies of ethylenediamine modified cellulose for removal of Cd and Pb. *Analytical Letters*, 44(11): 1925–1936.
- Nada A A M A, Hassan M L, 2006. Ion exchange properties of carboxylated bagasse. *Journal of Applied Polymer Science*, 102(2): 1399–1404.
- O'Connell D W, Birkinshaw C, O'Dwyer T F, 2008. Heavy metal adsorbents prepared from the modification of cellulose: A review. *Bioresource Technology*, 99(15): 6709–6724.

- Pagliuca A, Mufti G J, Baldwin D, Lestas A N, Wallis R M, Bellingham A J, 1990. Lead poisoning: clinical, biochemical, and haematological aspects of a recent outbreak. *Journal of Clinical Pathology*, 43(4): 277–281.
- Ren Y M, Li N, Feng J, Luan T Z, Wen Q, Li Z S et al., 2012. Adsorption of Pb(II) and Cu(II) from aqueous solution on magnetic porous ferromagnetic MnFe₂O₄. *Journal of Colloid and Interface Science*, 367(1): 415–421.
- Samir M A S A, Alloin F, Dufresne A, 2005. Review of recent research into cellulosic whiskers, their properties and their application in nanocomposite field. *Biomacromolecules*, 6(2): 612–626.
- Shen W, Chen S Y, Shi S K, Li X, Zhang X, Hu W L et al., 2009. Adsorption of Cu(II) and Pb(II) onto diethylenetriamine-bacterial cellulose. *Carbohydrate Polymers*, 75(1): 110–114.
- Taty-Costodes V C, Fauduet H, Porte C, Delacroix A, 2003. Removal of Cd(II) and Pb(II) ions, from aqueous solutions, by adsorption onto sawdust of *Pinus sylvestris*. *Journal of Hazardous Materials*, 105(1-3): 121–142.
- Xing S T, Zhao M Q, Ma Z C, 2011. Removal of heavy metal ions from aqueous solution using red loess as an adsorbent. *Journal of Environmental Sciences*, 23(9): 1497–1502.
- Zhao X W, Zhang G, Jia Q, Zhao C J, Zhou W H, Li W J, 2011. Adsorption of Cu(II), Pb(II), Co(II), Ni(II), and Cd(II) from aqueous solution by poly(aryl ether ketone) containing pendant carboxyl groups (PEK-L): Equilibrium, kinetics, and thermodynamics. *Chemical Engineering Journal*, 171(1): 152–158.
- Zheng J C, Feng H M, Lam M H W, Lam P K S, Ding Y W, Yu H Q, 2009. Removal of Cu(II) in aqueous media by biosorption using water hyacinth roots as a biosorbent material. *Journal of Hazardous Materials*, 171(1-3): 780–785.

JOURNAL OF ENVIRONMENTAL SCIENCES

环境科学学报(英文版)
(<http://www.jesc.ac.cn>)

Aims and scope

Journal of Environmental Sciences is an international academic journal supervised by Research Center for Eco-Environmental Sciences, Chinese Academy of Sciences. The journal publishes original, peer-reviewed innovative research and valuable findings in environmental sciences. The types of articles published are research article, critical review, rapid communications, and special issues.

The scope of the journal embraces the treatment processes for natural groundwater, municipal, agricultural and industrial water and wastewaters; physical and chemical methods for limitation of pollutants emission into the atmospheric environment; chemical and biological and phytoremediation of contaminated soil; fate and transport of pollutants in environments; toxicological effects of terrorist chemical release on the natural environment and human health; development of environmental catalysts and materials.

For subscription to electronic edition

Elsevier is responsible for subscription of the journal. Please subscribe to the journal via <http://www.elsevier.com/locate/jes>.

For subscription to print edition

China: Please contact the customer service, Science Press, 16 Donghuangchenggen North Street, Beijing 100717, China. Tel: +86-10-64017032; E-mail: journal@mail.sciencep.com, or the local post office throughout China (domestic postcode: 2-580).

Outside China: Please order the journal from the Elsevier Customer Service Department at the Regional Sales Office nearest you.

Submission declaration

Submission of an article implies that the work described has not been published previously (except in the form of an abstract or as part of a published lecture or academic thesis), that it is not under consideration for publication elsewhere. The submission should be approved by all authors and tacitly or explicitly by the responsible authorities where the work was carried out. If the manuscript accepted, it will not be published elsewhere in the same form, in English or in any other language, including electronically without the written consent of the copyright-holder.

Submission declaration

Submission of the work described has not been published previously (except in the form of an abstract or as part of a published lecture or academic thesis), that it is not under consideration for publication elsewhere. The publication should be approved by all authors and tacitly or explicitly by the responsible authorities where the work was carried out. If the manuscript accepted, it will not be published elsewhere in the same form, in English or in any other language, including electronically without the written consent of the copyright-holder.

Editorial

Authors should submit manuscript online at <http://www.jesc.ac.cn>. In case of queries, please contact editorial office, Tel: +86-10-62920553, E-mail: jesc@263.net, jesc@rcees.ac.cn. Instruction to authors is available at <http://www.jesc.ac.cn>.

Journal of Environmental Sciences (Established in 1989)

Vol. 25 No. 5 2013

Supervised by	Chinese Academy of Sciences	Published by	Science Press, Beijing, China
Sponsored by	Research Center for Eco-Environmental Sciences, Chinese Academy of Sciences		Elsevier Limited, The Netherlands
Edited by	Editorial Office of Journal of Environmental Sciences P. O. Box 2871, Beijing 100085, China Tel: 86-10-62920553; http://www.jesc.ac.cn E-mail: jesc@263.net , jesc@rcees.ac.cn	Distributed by	
		Domestic	Science Press, 16 Donghuangchenggen North Street, Beijing 100717, China Local Post Offices through China
		Foreign	Elsevier Limited http://www.elsevier.com/locate/jes
Editor-in-chief	Hongxiao Tang	Printed by	Beijing Beilin Printing House, 100083, China
CN 11-2629/X	Domestic postcode: 2-580		Domestic price per issue RMB ¥ 110.00

ISSN 1001-0742

